Correlated event-by-event fluctuations of flow harmonics in Pb-Pb collisions at √sNN=2.76 TeV

(ALICE Collaboration) Adam, J.; ...; Antičić, Tome; ...; Gotovac, Sven; ...; Erhardt, Filip; ...; Mudnić, Eugen; ...; ...

Correlated Event-by-Event Fluctuations of Flow Harmonics
in Pb-Pb Collisions at $\sqrt{s_{NN}} = 2.76$ TeV

J. Adam *et al.*[*]

(ALICE Collaboration)

(Received 4 May 2016; published 28 October 2016)

We report the measurements of correlations between event-by-event fluctuations of amplitudes of anisotropic flow harmonics in nucleus-nucleus collisions, obtained for the first time using a new analysis method based on multiparticle cumulants in mixed harmonics. This novel method is robust against systematic biases originating from nonflow effects and by construction any dependence on symmetry planes is eliminated. We demonstrate that correlations of flow harmonics exhibit a better sensitivity to medium properties than the individual flow harmonics. The new measurements are performed in Pb-Pb collisions at the center-of-mass energy per nucleon pair of $\sqrt{s_{NN}} = 2.76$ TeV by the ALICE experiment at the Large Hadron Collider. The centrality dependence of correlation between event-by-event fluctuations of the elliptic v_2 and quadrangular v_4 flow harmonics, as well as of anticorrelation between v_2 and triangular v_3 flow harmonics are presented. The results cover two different regimes of the initial state configurations: geometry dominated (in midcentral collisions) and fluctuation dominated (in the most central collisions). Comparisons are made to predictions from Monte Carlo Glauber, viscous hydrodynamics, AMPT, and HIJING models. Together with the existing measurements of the individual flow harmonics the presented results provide further constraints on the initial conditions and the transport properties of the system produced in heavy-ion collisions.

The properties of an extreme state of matter, the quark-gluon plasma (QGP), are studied by colliding heavy ions at BNL's Relativistic Heavy Ion Collider (RHIC) and at CERN's Large Hadron Collider (LHC). One of the most widely utilized physical phenomena in the exploration of QGP properties is collective anisotropic flow [1,2]. The large elliptic flow discovered at RHIC energies [3], which at the LHC energy of 2.76 TeV is 30% larger [4] and is recently reported in Ref. [5] to increase even further at 5.02 TeV, demonstrated that the QGP behaves like a strongly coupled liquid with a very small ratio of the shear viscosity to entropy density, η/s, which is close to a universal lower bound of $1/4\pi$ [6].

Anisotropic flow is traditionally quantified with harmonics v_n and corresponding symmetry plane angles ψ_n in the Fourier series decomposition of the particle azimuthal distribution (parametrized with azimuthal angle φ) in the plane transverse to the beam direction [7]:

$$\frac{dN}{d\varphi} \propto 1 + 2 \sum_{n=1}^{\infty} v_n \cos[n(\varphi - \psi_n)]. \qquad (1)$$

The shape of the intersecting zone of two identical heavy ions in noncentral collisions is approximately ellipsoidal. This initial anisotropy is transferred via interactions among constituents and the pressure gradients developed in the QGP medium to an observable final-state anisotropic emission of particles with respect to the symmetry plane(s) of the intersecting zone. The resulting anisotropic flow for such an idealized ellipsoidal geometry is determined solely by even Fourier harmonics v_{2n}, and only one symmetry plane (the reaction plane) exists. Recently, the importance of flow fluctuations and related additional observables has been identified. This has led to new concepts such as nonvanishing odd harmonics v_{2n-1} at midrapidity [8], nonidentical symmetry plane angles ψ_n and their intercorrelations [9–14], the stochastic nature of the harmonic v_n and its probability density function $P(v_n)$ [15–20], and, finally, the importance of higher order flow moments $\langle v_n^k \rangle$ (where the angular brackets denote an average over all events, and $k \geq 2$) [21]. Two distinct regimes for anisotropic flow development are nowadays scrutinized separately: geometry dominated (in midcentral collisions) and fluctuation dominated (in the most central collisions) [11].

Anisotropic flow is generated by the initial anisotropic geometry and its fluctuations coupled with an expansion of the produced medium. The initial coordinate space anisotropy can be quantified in terms of the eccentricity coefficients ε_n and the corresponding symmetry plane angles Φ_n [8,15,22]. A great deal of effort is being invested

---

to understand the relations between the momentum space Fourier harmonics v_n and the symmetry planes ψ_n on one side, and their spatial counterparts ε_n and Φ_n on the other side. These relations describe the response of the produced system to the initial coordinate space anisotropies, and therefore provide a rich repository of constraints for the system properties. In the early studies it was regularly assumed that, for small eccentricities, the harmonics v_n respond linearly to the eccentricities ε_n of the same order, $v_n \propto \varepsilon_n$, and that $\psi_n \simeq \Phi_n$ [8,10,23,24]. However, for sizable eccentricities recent studies argue that the anisotropies in momentum and coordinate space are related instead with the matrix equation connecting a set of anisotropic flow harmonics $\{v_n\}$ and a set of eccentricity coefficients $\{\varepsilon_n\}$; it was demonstrated that the hydrodynamic response is both nondiagonal and nonlinear, and that in general $\psi_n \neq \Phi_n$ [9,11,25,26]. The first realization led to the conclusion that a relationship between event-by-event fluctuations of the amplitudes of two different flow harmonics v_m and v_n can exist. This is hardly surprising for even flow harmonics in noncentral collisions because the ellipsoidal shape generates nonvanishing values for all even harmonics v_{2n} [27], not only for elliptic flow. However, this simple geometrical argument cannot explain the possible relation between the even and odd flow harmonics in noncentral collisions, and the argument is not applicable in the central collisions, where all initial shapes are equally probable since they originate solely from fluctuations. Recently a linear correlation coefficient $c(a, b)$ was defined in this context, which becomes 1 (−1) if observables a and b are fully linearly (antilinearly) correlated and zero in the absence of correlation [25]. Model calculations of this new observable showed that neither v_2 and v_3 nor v_2 and v_4 are linearly correlated in noncentral collisions. Most importantly, it was demonstrated that $c(v_2, v_4)$ depends strongly both on η/s of the QGP and on the value of $c(\varepsilon_2, \varepsilon_4)$, which quantifies the relationship between corresponding eccentricities in the initial state [25]. Therefore, it was concluded that new observables $c(v_n, v_m)$, depending on the choice of flow harmonics v_n and v_m, are sensitive both to the fluctuations of the initial conditions and to the transport properties of the QGP, with the potential to discriminate between the two respective contributions when combined with a measurement of individual flow harmonics [25].

In this Letter we study the relationship between event-by-event fluctuations of magnitudes of two different flow harmonics of order n and m by using a recently proposed four-particle observable [28]:

$$\langle\langle\cos(m\varphi_1 + n\varphi_2 - m\varphi_3 - n\varphi_4)\rangle\rangle_c = \langle\langle\cos(m\varphi_1 + n\varphi_2 - m\varphi_3 - n\varphi_4)\rangle\rangle$$
$$- \langle\langle\cos[m(\varphi_1 - \varphi_2)]\rangle\rangle\langle\langle\cos[n(\varphi_1 - \varphi_2)]\rangle\rangle$$
$$= \langle v_m^2 v_n^2 \rangle - \langle v_m^2 \rangle\langle v_n^2 \rangle \tag{2}$$

with the condition $m \neq n$ for two positive integers m and n. We refer to these new observables as the symmetric two-harmonic four-particle cumulant, and use the notation SC(m, n), or just SC. The double angular brackets indicate that the averaging procedure has been performed in two steps—first, averaging over all distinct particle quadruplets in an event, and then in the second step weighting the single-event averages with the "number of combinations." The latter for single-event average four-particle correlations is mathematically equivalent to a unit weight for each individual quadruplet when the multiplicity differs event by event [29]. In both two-particle correlators above all distinct particle pairs are considered in each case. The four-particle cumulant in Eq. (2) is less sensitive to nonflow correlations than any two- or four-particle correlator on the right-hand side taken individually [30,31]. The last equality is true only in the absence of nonflow effects [32]. The observable in Eq. (2) is zero in the absence of flow fluctuations, or if the magnitudes of the harmonics v_m and v_n are uncorrelated [28]. It is also unaffected by the relationship between the symmetry plane angles ψ_m and ψ_n. The four-particle cumulant in Eq. (2) is proportional to the linear correlation coefficient $c(a, b)$ introduced in Ref. [25] and discussed above, with $a = v_m^2$ and $b = v_n^2$. Experimentally, it is more reliable to measure the higher order moments of the flow harmonics $v_n^k (k \geq 2)$ with two- and multiparticle correlation techniques [31,33,34], than to measure the first moments v_n with the event plane method, due to the systematic uncertainties involved in the event-by-event estimation of the symmetry planes [35,36]. Therefore, we have used the new multiparticle observable in Eq. (2) as meant to be the least biased measure of the correlation between event-by-event fluctuations of magnitudes of the two different harmonics v_m and v_n [28].

The two- and four-particle correlations in Eq. (2) were evaluated in terms of Q vectors [33]. The Q vector (or flow vector) in harmonic n for a set of M particles, where throughout this Letter M is the multiplicity of an event, is defined as $Q_n \equiv \sum_{k=1}^{M} e^{in\varphi_k}$ [7,37]. We have used for a single-event average two-particle correlation $\langle\cos(n(\varphi_1 - \varphi_2))\rangle$ the following definition and analytic result in terms of Q vectors:

$$\frac{1}{\binom{M}{2}2!} \sum_{\substack{i,j=1 \\ (i \neq j)}}^{M} e^{in(\varphi_i - \varphi_j)} = \frac{1}{\binom{M}{2}2!}[|Q_n|^2 - M]. \tag{3}$$

For four-particle correlation $\langle\cos(m\varphi_1 + n\varphi_2 - m\varphi_3 - n\varphi_4)\rangle$ we used

$$\frac{1}{\binom{M}{4}4!}\sum_{\substack{i,j,k,l=1\\(i\neq j\neq k\neq l)}}^{M} e^{i(m\varphi_i + n\varphi_j - m\varphi_k - n\varphi_l)} = \frac{1}{\binom{M}{4}4!}\{|Q_m|^2|Q_n|^2 - 2\text{Re}[Q_{m+n}Q_m^*Q_n^*] - 2\text{Re}[Q_mQ_{m-n}^*Q_n^*]$$

$$+ |Q_{m+n}|^2 + |Q_{m-n}|^2 - (M-4)(|Q_m|^2 + |Q_n|^2) + M(M-6)\}. \tag{4}$$

In order to obtain the all-event average correlations, denoted by $\langle\langle\cdots\rangle\rangle$ in Eq. (2), we have weighted single-event expressions in Eqs. (3) and (4) with weights $M(M-1)$ and $M(M-1)(M-2)(M-3)$, respectively [29].

The data used in this analysis were obtained with the ALICE detector [38,39]. They consist of minimum-bias Pb-Pb collisions recorded during the 2010 LHC Pb-Pb run at $\sqrt{s_{NN}} = 2.76$ TeV. With the default event and track selection criteria described below, we have obtained in total about 1.8×10^5 events per 1% centrality bin width. All individual systematic variations were combined in quadrature to obtain the final uncertainty.

The centrality was determined with the V0 detector [40–42]. As a part of systematic checks the centrality was determined independently with the time projection chamber (TPC) [43] and the silicon pixel detector [44,45], which have slightly worse resolution [42]. A systematic difference of up to 3% was observed in the $\text{SC}(m,n)$ results when using different centrality estimations. Charged particles were reconstructed with the TPC and the inner tracking system [44,45] immersed in a 0.5 T solenoidal field. The TPC is capable of detecting charged particles in the transverse momentum range $0.1 < p_T < 100$ GeV/c, with a p_T resolution of less than 6% for tracks below 20 GeV/c. Because of TPC dead zones between neighboring sectors, the track finding efficiency is about 75% for $p_T = 200$ MeV/c and then it saturates at about 85% for $p_T > 1$ GeV/c in Pb-Pb collisions. The TPC covers the full azimuth and has a pseudorapidity coverage of $|\eta| < 0.9$. Tracks reconstructed using the TPC and inner tracking system are referred to as global, while tracks reconstructed only with the TPC are referred to as TPC only.

For online triggering, the V0 and silicon pixel detectors were used [39]. The reconstructed primary vertex is required to lie within ± 10 cm of the nominal interaction point in the longitudinal direction along the beam axis. The cut on the position of the primary vertex along the beam axis was varied from ± 12 to ± 6 cm; the resulting SC measurements are consistent with those obtained with the default cut.

The main analysis was performed with global tracks selected in the transverse momentum interval $0.2 < p_T < 5.0$ GeV/c and the pseudorapidity region $|\eta| < 0.8$. With this choice of a low p_T cutoff we are reducing event-by-event biases from a smaller reconstruction efficiency at lower p_T, while the high p_T cutoff was introduced to reduce the contribution to the anisotropies from the jets.

Reconstructed tracks were required to have at least 70 TPC space points (out of a maximum of 159). Only tracks with a transverse distance of closest approach (DCA) to the primary vertex less than 3 mm are accepted to reduce the contamination from secondary tracks. Tracks with kinks (the tracks that appear to change direction due to multiple scattering, $K^\pm$ decays) were rejected.

An independent analysis was performed with TPC-only and hybrid tracks (see below). For TPC-only tracks, the DCA cut was relaxed to 3 cm, providing a different sensitivity to contamination from the secondary tracks. Both the azimuthal acceptance and the reconstruction efficiency as a function of transverse momentum differ between the TPC-only and global tracks. The resulting difference between independent analyses with global and TPC-only tracks was found to be 1%–5% in all the centrality ranges studied, both for SC(3,2) and SC(4,2). In another independent analysis with hybrid tracks, three different types of tracks were combined, in order to overcome the nonuniform azimuthal acceptance due to dead zones in the silicon pixel detector, and to achieve the best transverse momentum resolution [39]. In this analysis the DCA cut was set to 3.2 cm in the longitudinal and to 2.4 cm in the transverse direction. The results between the global and hybrid tracks differ by 3% to 5%, depending on the observable considered.

One of the largest contributions to the systematic uncertainty originates from the nonuniform reconstruction efficiency as a function of transverse momentum. For the observables SC(3,2) and SC(4,2) the uncertainty is 7% and 8%, respectively. In order to correct the measurements of these azimuthal correlators for various detector inefficiencies, we have constructed the particle weights as a function of azimuthal angle φ and transverse momentum p_T, and used the prescription outlined in Ref. [28]. In particular, p_T weights were constructed as a ratio of the transverse momentum distribution obtained from Monte Carlo generated tracks and from tracks reconstructed after they have passed through the detector simulated with GEANT3 [46].

We have used four Monte Carlo models in this Letter. The HIJING model [47,48] was utilized to obtain the p_T weights [28]. Second, the HIJING model was used to estimate the strength of the nonflow correlations (typically few-particle correlations insensitive to the collision geometry). We have evaluated the observables of interest in coordinate space by modeling the initial conditions with a Monte Carlo Glauber model [49]. We have compared the
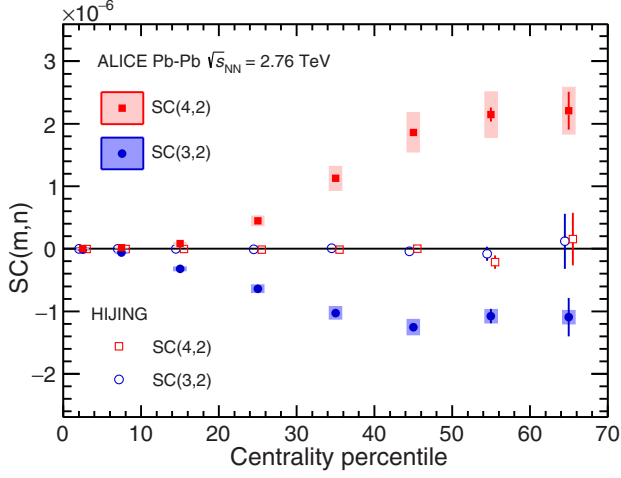
FIG. 1.   Centrality dependence of the observables SC(4,2) (red filled squares) and SC(3,2) (blue filled circles) in Pb-Pb collisions at 2.76 TeV. Systematic errors are represented with boxes. The results for the HIJING model are shown with hollow markers.

centrality dependence of our observables with the theoretical model from Ref. [50], where the initial energy density profiles are calculated using a next-to-leading order perturbative-QCD+saturation model [51,52]. The subsequent spacetime evolution is described by relativistic dissipative fluid dynamics with different parametrizations for the temperature dependence of the shear viscosity to entropy density ratio $\eta/s(T)$. Each of the $\eta/s(T)$ parametrizations is adjusted to reproduce the measured v_n from central to midperipheral collisions. Finally, we provide an independent estimate of the centrality dependence of our observables by utilizing the AMPT model [53].

The centrality dependence of SC(4,2) (red squares) and SC(3,2) (blue circles) is presented in Fig. 1. Positive values of SC(4,2) are observed for all centralities. This suggests a correlation between the event-by-event fluctuations of v_2 and v_4, which indicates that finding v_2 larger than $\langle v_2 \rangle$ in an event enhances the probability of finding v_4 larger than $\langle v_4 \rangle$ in that event. On the other hand, the negative results of SC(3,2) show the anticorrelation between the v_2 and v_3 magnitudes, which further imply that finding v_2 larger than $\langle v_2 \rangle$ enhances the probability of finding v_3 smaller than $\langle v_3 \rangle$. We have calculated the SC observables using HIJING, which does not include anisotropic collectivity but, e.g., azimuthal correlations due to jet production [47,48]. It is found that in HIJING both $\langle\langle \cos(m\varphi_1 + n\varphi_2 - m\varphi_3 - n\varphi_4) \rangle\rangle$ and $\langle\langle \cos[m(\varphi_1 - \varphi_2)] \rangle\rangle\langle\langle \cos[n(\varphi_1 - \varphi_2)] \rangle\rangle$ are nonzero. However, the calculated SC observables from HIJING are compatible with zero for all centralities, which suggests that the SC measurements are nearly insensitive to nonflow correlations. We have also performed a study using the like-sign technique, which is another powerful approach to estimate the nonflow effects [4]. It was found that the difference between the correlations for like-sign and all charged combinations is within 10%. This demonstrates
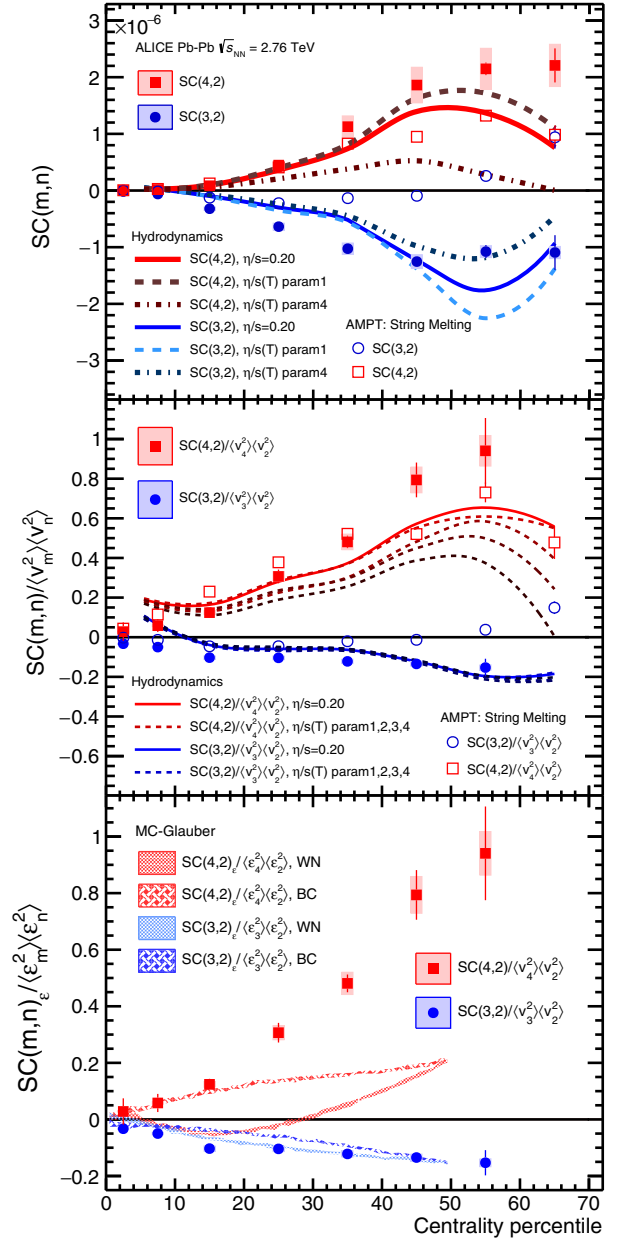

FIG. 2.   AMPT model predictions are shown as hollow symbols in the (top) and (middle) panels. Top: comparison of the observables SC(4,2) (red filled squares) and SC(3,2) (blue filled circles) to the theoretical model from Ref. [50]. The solid lines indicate the predictions with constant η/s, while the dashed lines indicate predictions for different parametrizations of the η/s temperature dependence (labeled in the same way as in Fig. 1 in Ref. [50]). Middle: results divided by $\langle v_m^2 \rangle\langle v_n^2 \rangle$. Bottom: comparison to the Monte Carlo Glauber model using wounded nucleon (WN) and binary collision (BC) weights.

that nonzero values of SC measurements cannot be explained by nonflow effects.

A study based on the AMPT model showed that the observed (anti)correlations are also sensitive to the transport properties, e.g., the partonic and hadronic interactions [20,28]. Figure 2 shows the comparison of SC(3,2) and

SC(4,2) to the AMPT calculations, which generally predict the correct sign but underestimate their magnitude. The comparison between experimental data and the theoretical calculations [50], which incorporate both the initial conditions and the system evolution, is shown in Fig. 2 (top). The model captures qualitatively the centrality dependence, but not quantitatively. Most notably, there is no single centrality for which a given $\eta/s(T)$ parametrization describes simultaneously both SC(4,2) and SC(3,2). On the other hand, the same theoretical model captures quantitatively the centrality dependence of the individual v_2, v_3, and v_4 harmonics with a precision better than 10% in the central and midcentral collisions [50]. We therefore conclude that the individual flow harmonics v_n and new SC(m,n) observables together provide a better handle on the initial conditions and $\eta/s(T)$ than each of them alone. This is emphasized in Fig. 2 (middle), where the SC(3,2) and SC(4,2) observables were divided with the products $\langle v_3^2\rangle\langle v_2^2\rangle$ and $\langle v_4^2\rangle\langle v_2^2\rangle$, respectively, in order to obtain the normalized SC observables (the result for 60%–70% is omitted due to the large statistical uncertainty). These products were obtained with two-particle correlations and using a pseudorapidity gap of $|\Delta\eta| > 1.0$ to suppress biases from few-particle nonflow correlations. We have found that the normalized SC(4,2) observable exhibits much better sensitivity to different $\eta/s(T)$ parametrizations than the normalized SC(3,2) observable, see Fig. 2 (middle), and than the individual flow harmonics [50]. These findings indicate that the normalized SC(3,2) observable is sensitive mainly to the initial conditions, while the normalized SC(4,2) observable is sensitive to both the initial conditions and the system properties, which is consistent with the prediction from Ref. [25].

It can be seen in Fig. 1 that SC(4,2) and SC(3,2) increase nonlinearly up to centrality 60%. Assuming only a linear response, $v_n \propto \varepsilon_n$, we expect that the normalized SC(m,n) evaluated in coordinate space can capture the measurement of the centrality dependence of the normalized SC(m,n) in the momentum space. The correlations between the nth and mth order harmonics were estimated with calculations of $(\langle \varepsilon_n^2\varepsilon_m^2\rangle - \langle\varepsilon_n^2\rangle\langle\varepsilon_m^2\rangle)/\langle\varepsilon_n^2\rangle\langle\varepsilon_m^2\rangle$, i.e., a normalized SC observable in the coordinate space, which we denote SC($m,n)_\varepsilon/\langle\varepsilon_n^2\rangle\langle\varepsilon_m^2\rangle$. Here, ε_n (ε_m) is the nth (mth) order coordinate space anisotropy, following the definition in Ref. [8]. Different scenarios of the Monte Carlo Glauber model, named the wounded nucleon and binary collision weights, have been used. An increasing trend from central to peripheral collisions with different sign has been observed in Fig. 2 (bottom) for SC(4,2) and SC(3,2). A dramatic deviation of SC(4,2) between data and the model calculation is observed for noncentral collisions. This deviation increases from midcentral to peripheral, which could be understood as the contribution of the nonlinear response (ε_2 contributes to v_4) increasing as a function of centrality, which is consistent with that reported

in Ref. [54]. Since the normalized SC(3,2) appears to be sensitive only to the initial conditions and not to $\eta/s(T)$, see Fig. 2 (middle), the Monte Carlo Glauber model captures better its centrality dependence than it does for the normalized SC(4,2) observable, see Fig. 2 (bottom).

The relationship between the flow harmonics v_2, v_3, v_4 has also been investigated by the ATLAS Collaboration using the event shape engineering technique [54–56]. For events with a larger v_2, the ATLAS Collaboration showed these have a smaller than average v_3, and a larger than average v_4. For events with a smaller v_2, the opposite trend occurred. These observations are consistent with the patterns observed via the SC measurements presented in this Letter. The SC observables, however, provide a compact quantitative measure of these correlations, without fitting correlations between v_n and v_m. This simplifies the quantitative comparison of the SC observables with hydrodynamical calculations as shown in Fig. 2.

In the most central collisions the anisotropies originate mainly from fluctuations; i.e., the initial ellipsoidal
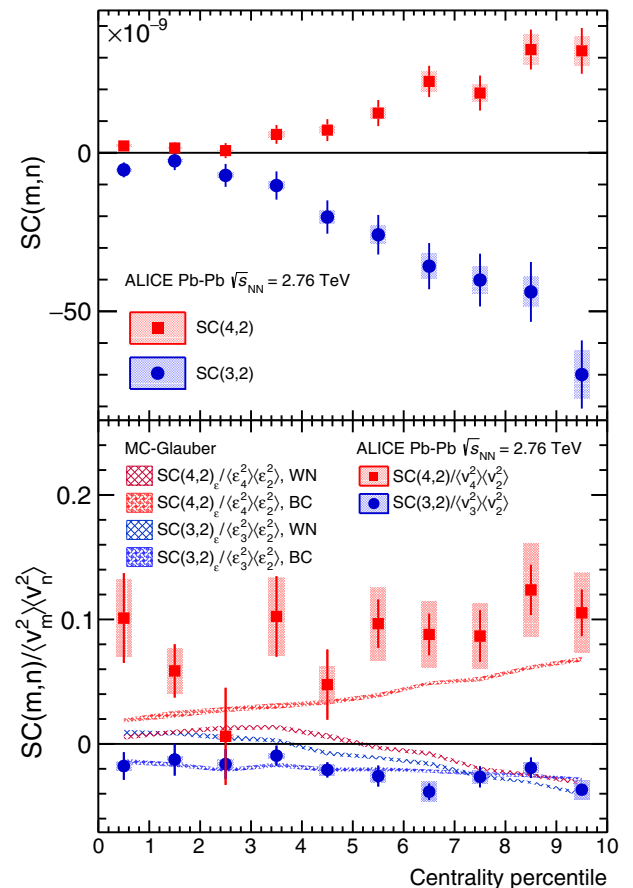

FIG. 3. Top: correlated and anticorrelated event-by-event fluctuations in coordinate (Monte Carlo Glauber model) and momentum space (data). Bottom: normalized SC observables, where the pseudorapidity gap $|\Delta\eta| > 1.0$ was applied in both two-particle correlations in the denominator used to estimate the individual flow harmonics.

geometry characteristic for midcentral collisions plays little role in this regime. Therefore, we have performed a separate analysis for the centrality range 0%–10% in centrality bins of 1%. The results are presented in Fig. 3. We observe that event-by-event fluctuations of v_2 and v_4 remain correlated, and of v_2 and v_3 anticorrelated, also in this regime. However, the strength of the (anti) correlations exhibits a different centrality dependence than for the wider centrality range shown in Fig. 1. As seen in Fig. 3 (top) the centrality dependence cannot be linearly extrapolated from the 0%–10% region to the full centrality range. Comparison with the two different parametrizations of the Monte Carlo Glauber initial conditions for the normalized SC observables presented in Fig. 3 (bottom) suggests that the binary collision parametrization (binary collision weights) is favored by the data in most central collisions. This agreement may suggest the scaling with the number of quark participants [57–61] in central collisions at the LHC energies.

In summary, we have measured for the first time the new multiparticle observables, the symmetric two-harmonic four-particle cumulants, which quantify the relationship between the event-by-event fluctuations of two different flow harmonics. We have found that the fluctuations of v_2 and v_3 are anticorrelated in all centralities; however, the details of the centrality dependence differ in the fluctutation-dominated (most central) and the geometry-dominated (midcentral) regimes. The fluctuations of v_2 and v_4 are correlated for all centralities. The SC observables were used to discriminate between the state-of-the-art hydro model calculations with different parametrizations of the temperature dependence of η/s, for all of which the centrality dependence of elliptic, triangular, and quadrangular flow has a weaker sensitivity at the LHC. In particular, the centrality dependence of SC(4,2) cannot be captured with the constant η/s. We have also used our results to discriminate between two different parametrizations of the initial conditions and have demonstrated that in the fluctuation-dominated regime (in central collisions) the Monte Carlo Glauber initial conditions with binary collision weights are favored over wounded nucleon weights.

[1] J.-Y. Ollitrault, Anisotropy as a signature of transverse collective flow, Phys. Rev. D **46**. 229 (1992).

[2] S. A. Voloshin, A. M. Poskanzer, and R. Snellings, Collective phenomena in noncentral nuclear collisions, arXiv:0809.2949.

[3] K. H. Ackermann *et al.* (STAR Collaboration), Elliptic Flow in Au + Au Collisions at $\sqrt{s_{NN}} = 130$ GeV, Phys. Rev. Lett. **86**, 402 (2001).

[4] K. Aamodt *et al.* (ALICE Collaboration), Elliptic Flow of Charged Particles in Pb-Pb Collisions at 2.76 TeV, Phys. Rev. Lett. **105**, 252302 (2010).

[5] J. Adam *et al.* (ALICE Collaboration), Anisotropic Flow of Charged Particles in Pb-Pb Collisions at $\sqrt{s_{NN}} = 5.02$ TeV, Phys. Rev. Lett. **116**, 132302 (2016).

[6] P. K. Kovtun, D. T. Son, and A. O. Starinets, Viscosity in Strongly Interacting Quantum Field Theories from Black Hole Physics, Phys. Rev. Lett. **94**, 111601 (2005).

[7] S. Voloshin and Y. Zhang, Flow study in relativistic nuclear collisions by Fourier expansion of azimuthal particle distributions, Z. Phys. C **70**, 665 (1996).

[8] B. Alver and G. Roland, Collision geometry fluctuations and triangular flow in heavy-ion collisions, Phys. Rev. C **81**, 054905 (2010); **82**, 039903(E) (2010).

[9] G.-Y. Qin, H. Petersen, S. A. Bass, and B. Muller, Translation of collision geometry fluctuations into momentum anisotropies in relativistic heavy-ion collisions, Phys. Rev. C **82**, 064903 (2010).

[10] D. Teaney and L. Yan, Triangularity and dipole asymmetry in heavy ion collisions, Phys. Rev. C **83**, 064904 (2011).

[11] Z. Qiu and U. W. Heinz, Event-by-event shape and flow fluctuations of relativistic heavy-ion collision fireballs, Phys. Rev. C **84**, 024911 (2011).

[12] K. Aamodt *et al.* (ALICE Collaboration), Higher Harmonic Anisotropic Flow Measurements of Charged Particles in Pb-Pb Collisions at $\sqrt{s_{NN}} = 2.76$ TeV, Phys. Rev. Lett. **107**, 032301 (2011).

[13] A. Adare *et al.* (PHENIX Collaboration), Measurements of Higher-Order Flow Harmonics in Au + Au Collisions at $\sqrt{s_{NN}} = 200$ GeV, Phys. Rev. Lett. **107**, 252301 (2011).

[14] G. Aad *et al.* (ATLAS Collaboration), Measurement of event-plane correlations in $\sqrt{s_{NN}} = 2.76$ TeV lead-lead collisions with the ATLAS detector, Phys. Rev. C **90**, 024905 (2014).

[15] S. A. Voloshin, A. M. Poskanzer, A. Tang, and G. Wang, Elliptic flow in the Gaussian model of eccentricity fluctuations, Phys. Lett. B **659**, 537 (2008).

[16] C. Gale, S. Jeon, B. Schenke, P. Tribedy, and R. Venugopalan, Initial state fluctuations and higher harmonic flow in heavy-ion collisions, Nucl. Phys. **A904–905**, 409c (2013).

[17] G. Aad *et al.* (ATLAS Collaboration), Measurement of the distributions of event-by-event flow harmonics in lead-lead collisions at $\sqrt{s_{NN}} = 2.76$ TeV with the ATLAS detector at the LHC, J. High Energy Phys. 11 (2013) 183.

[18] L. Yan and J.-Y. Ollitrault, Universal Fluctuation-Driven Eccentricities in Proton-Proton, Proton-Nucleus and Nucleus-Nucleus Collisions, Phys. Rev. Lett. **112**, 082301 (2014).

[19] L. Yan, J.-Y. Ollitrault, and A. M. Poskanzer, Eccentricity distributions in nucleus-nucleus collisions, Phys. Rev. C **90**, 024903 (2014).

[20] Y. Zhou, K. Xiao, Z. Feng, F. Liu, and R. Snellings, Anisotropic distributions in a multi-phase transport model, Phys. Rev. C **93**, 034909 (2016).

[21] R. S. Bhalerao, J.-Y. Ollitrault, and S. Pal, Characterizing flow fluctuations with moments, Phys. Lett. B **742**, 94 (2015).

[22] B. Alver *et al.* (PHOBOS Collaboration), System Size, Energy, Pseudorapidity, and Centrality Dependence of Elliptic Flow, Phys. Rev. Lett. **98**, 242302 (2007).

[23] B. H. Alver, C. Gombeaud, M. Luzum, and J.-Y. Ollitrault, Triangular flow in hydrodynamics and transport theory, Phys. Rev. C **82**, 034913 (2010).

[24] R. A. Lacey, D. Reynolds, A. Taranenko, N. N. Ajitanand, J. M. Alexander, F.-H. Liu, Y. Gu, and A. Mwai, Acoustic scaling of anisotropic flow in shape-engineered events: Implications for extraction of the specific shear viscosity of the quark gluon plasma, arXiv:1311.1728.

[25] H. Niemi, G. S. Denicol, H. Holopainen, and P. Huovinen, Event-by-event distributions of azimuthal asymmetries in ultrarelativistic heavy-ion collisions, Phys. Rev. C **87**, 054901 (2013).

[26] L. Yan and J.-Y. Ollitrault, $\nu_4, \nu_5, \nu_6, \nu_7$: Nonlinear hydrodynamic response versus LHC data, Phys. Lett. B **744**, 82 (2015).

[27] P. F. Kolb, v_4: A Small, but sensitive observable for heavy ion collisions, Phys. Rev. C **68**, 031902 (2003).

[28] A. Bilandzic, C. H. Christensen, K. Gulbrandsen, A. Hansen, and Y. Zhou, Generic framework for anisotropic flow analyses with multiparticle azimuthal correlations, Phys. Rev. C **89**, 064904 (2014).

[29] A. Bilandzic, Ph.D. thesis, Utrecht U., 2012, https://inspirehep.net/record/1186272/files/CERN-THESIS-2012-018.pdf.

[30] N. Borghini, P. M. Dinh, and J.-Y. Ollitrault, A new method for measuring azimuthal distributions in nucleus-nucleus collisions, Phys. Rev. C **63**, 054906 (2001).

[31] N. Borghini, P. M. Dinh, and J.-Y. Ollitrault, Flow analysis from multiparticle azimuthal correlations, Phys. Rev. C **64**, 054901 (2001).

[32] R. S. Bhalerao, M. Luzum, and J.-Y. Ollitrault, Determining initial-state fluctuations from flow measurements in heavy-ion collisions, Phys. Rev. C **84**, 034910 (2011).

[33] A. Bilandzic, R. Snellings, and S. Voloshin, Flow analysis with cumulants: Direct calculations, Phys. Rev. C **83**, 044913 (2011).

[34] S. Wang, Y. Z. Jiang, Y. M. Liu, D. Keane, D. Beavis, S. Y. Chu, S. Y. Fung, M. Vient, C. Hartnack, and H. Stocker, Measurement of collective flow in heavy ion collisions using particle pair correlations, Phys. Rev. C **44**, 1091 (1991).

[35] A. M. Poskanzer and S. A. Voloshin, Methods for analyzing anisotropic flow in relativistic nuclear collisions, Phys. Rev. C **58**, 1671 (1998).

[36] M. Luzum and J.-Y. Ollitrault, Eliminating experimental bias in anisotropic-flow measurements of high-energy nuclear collisions, Phys. Rev. C **87**, 044907 (2013).

[37] J. Barrette *et al.* (E877 Collaboration), Observation of Anisotropic Event Shapes and Transverse Flow in Au + Au Collisions at AGS Energy, Phys. Rev. Lett. **73**, 2532 (1994).

[38] K. Aamodt *et al.* (ALICE Collaboration), The ALICE experiment at the CERN LHC, J. Instrum. **3**, S08002 (2008).

[39] B. B. Abelev *et al.* (ALICE Collaboration), Performance of the ALICE Experiment at the CERN LHC, Int. J. Mod. Phys. A **29**, 1430044 (2014).

[40] P. Cortese *et al.* (ALICE Collaboration), Report No. CERN-LHCC-2004-025, https://cds.cern.ch/record/781854/files/lhcc-2004-025.pdf.

[41] E. Abbas *et al.* (ALICE Collaboration), Performance of the ALICE VZERO system, J. Instrum. **8**, P10016 (2013).

[42] B. Abelev *et al.* (ALICE Collaboration), Centrality determination of Pb-Pb collisions at $\sqrt{s_{NN}} = 2.76$ TeV with ALICE, Phys. Rev. C **88**, 044909 (2013).

[43] J. Alme *et al.*, The ALICE TPC, a large 3-dimensional tracking device with fast readout for ultra-high multiplicity events, Nucl. Instrum. Methods Phys. Res., Sect. A **622**, 316 (2010).

[44] G. Dellacasa *et al.* (ALICE Collaboration), Report No. CERN-LHCC-99-12, https://cds.cern.ch/record/391175?ln=en.

[45] K. Aamodt *et al.* (ALICE Collaboration), Alignment of the ALICE Inner Tracking System with cosmic-ray tracks, J. Instrum. **5**, P03003 (2010).

[46] R. Brun, F. Carminati, and S. Giani, Report No. CERN-W5013, 1994, https://cds.cern.ch/record/1082634/files/geantall_CERN-W5013.pdf.

[47] X.-N. Wang and M. Gyulassy, HIJING: A Monte Carlo model for multiple jet production in pp, pA and AA collisions, Phys. Rev. D **44**, 3501 (1991).

[48] M. Gyulassy and X.-N. Wang, HIJING 1.0: A Monte Carlo program for parton and particle production in high-energy hadronic and nuclear collisions, Comput. Phys. Commun. **83**, 307 (1994).

[49] M. L. Miller, K. Reygers, S. J. Sanders, and P. Steinberg, Glauber modeling in high energy nuclear collisions, Annu. Rev. Nucl. Part. Sci. **57**, 205 (2007).

[50] H. Niemi, K. J. Eskola, and R. Paatelainen, Event-by-event fluctuations in perturbative QCD + saturation + hydro model: pinning down QCD matter shear viscosity in ultra-relativistic heavy-ion collisions, Phys. Rev. C **93**, 024907 (2016).

[51] R. Paatelainen, K. J. Eskola, H. Holopainen, and K. Tuominen, Multiplicities and p_T spectra in ultrarelativistic heavy ion collisions from a next-to-leading order improved perturbative QCD + saturation + hydrodynamics model, Phys. Rev. C **87**, 044904 (2013).

[52] R. Paatelainen, K. J. Eskola, H. Niemi, and K. Tuominen, Fluid dynamics with saturated minijet initial conditions in ultrarelativistic heavy-ion collisions, Phys. Lett. B **731**, 126 (2014).

[53] Z.-W. Lin, C. M. Ko, B.-A. Li, B. Zhang, and S. Pal, A Multi-phase transport model for relativistic heavy ion collisions, Phys. Rev. C **72**, 064901 (2005).

[54] G. Aad *et al.* (ATLAS Collaboration), Measurement of the correlation between flow harmonics of different order in lead-lead collisions at $\sqrt{s_{NN}} = 2.76$ TeV with the ATLAS detector, Phys. Rev. C **92**, 034903 (2015).

[55] J. Schukraft, A. Timmins, and S. A. Voloshin, Ultra-relativistic nuclear collisions: Event shape engineering, Phys. Lett. B **719**, 394 (2013).

[56] H. Petersen and B. Muller, Possibility of event shape selection in relativistic heavy ion collisions, Phys. Rev. C **88**, 044918 (2013).

[57] S. Eremin and S. Voloshin, Nucleon participants or quark participants?, Phys. Rev. C **67**, 064905 (2003).

[58] M. Miller and R. Snellings, Eccentricity fluctuations and its possible effect on elliptic flow measurements, arXiv:nucl-ex/0312008.

[59] L. Adamczyk *et al.* (STAR Collaboration), Azimuthal anisotropy in U + U and Au + Au collisions at RHIC, Phys. Rev. Lett. **115**, 222301 (2015).

[60] A. Adare *et al.* (PHENIX Collaboration), Transverse energy production and charged-particle multiplicity at midrapidity in various systems from $\sqrt{s_{NN}} = 7.7$ to 200 GeV, Phys. Rev. C **93**, 024901 (2016).

[61] C. Loizides, Glauber modeling of high-energy nuclear collisions at sub-nucleon level, Phys. Rev. C **94**, 024914 (2016).

J. Adam,[39] D. Adamová,[85] M. M. Aggarwal,[89] G. Aglieri Rinella,[35] M. Agnello,[111] N. Agrawal,[48] Z. Ahammed,[134] S. Ahmad,[18] S. U. Ahn,[69] S. Aiola,[138] A. Akindinov,[55] S. N. Alam,[134] D. S. D. Albuquerque,[122] D. Aleksandrov,[81] B. Alessandro,[111] D. Alexandre,[102] R. Alfaro Molina,[64] A. Alici,[12,105] A. Alkin,[3] J. R. M. Almaraz,[120] J. Alme,[22,37] T. Alt,[42] S. Altinpinar,[22] I. Altsybeev,[133] C. Alves Garcia Prado,[121] C. Andrei,[79] A. Andronic,[98] V. Anguelov,[94] T. Antičić,[99] F. Antinori,[108] P. Antonioli,[105] L. Aphecetche,[114] H. Appelshäuser,[61] S. Arcelli,[27] R. Arnaldi,[111] O. W. Arnold,[36,95]

I. C. Arsene,[21] M. Arslandok,[61] B. Audurier,[114] A. Augustinus,[35] R. Averbeck,[98] M. D. Azmi,[18] A. Badalà,[107] Y. W. Baek,[68] S. Bagnasco,[111] R. Bailhache,[61] R. Bala,[92] S. Balasubramanian,[138] A. Baldisseri,[15] R. C. Baral,[58] A. M. Barbano,[26] R. Barbera,[28] F. Barile,[32] G. G. Barnaföldi,[137] L. S. Barnby,[35,102] V. Barret,[71] P. Bartalini,[7] K. Barth,[35] J. Bartke,[118,†] E. Bartsch,[61] M. Basile,[27] N. Bastid,[71] S. Basu,[134] B. Bathen,[62] G. Batigne,[114] A. Batista Camejo,[71] B. Batyunya,[67] P. C. Batzing,[21] I. G. Bearden,[82] H. Beck,[61,94] C. Bedda,[111] N. K. Behera,[49,51] I. Belikov,[65] F. Bellini,[27] H. Bello Martinez,[2] R. Bellwied,[123] R. Belmont,[136] E. Belmont-Moreno,[64] L. G. E. Beltran,[120] V. Belyaev,[76] G. Bencedi,[137] S. Beole,[26] I. Berceanu,[79] A. Bercuci,[79] Y. Berdnikov,[87] D. Berenyi,[137] R. A. Bertens,[54] D. Berzano,[35] L. Betev,[35] A. Bhasin,[92] I. R. Bhat,[92] A. K. Bhati,[89] B. Bhattacharjee,[44] J. Bhom,[118,129] L. Bianchi,[123] N. Bianchi,[73] C. Bianchin,[136] J. Bielčík,[39] J. Bielčíková,[85] A. Bilandzic,[36,82,95] G. Biro,[137] R. Biswas,[4] S. Biswas,[4,80] S. Bjelogrlic,[54] J. T. Blair,[119] D. Blau,[81] C. Blume,[61] F. Bock,[75,94] A. Bogdanov,[76] H. Bøggild,[82] L. Boldizsár,[137] M. Bombara,[40] J. Book,[61] H. Borel,[15] A. Borissov,[97] M. Borri,[84,125] F. Bossú,[66] E. Botta,[26] C. Bourjau,[82] P. Braun-Munzinger,[98] M. Bregant,[121] T. Breitner,[60] T. A. Broker,[61] T. A. Browning,[96] M. Broz,[39] E. J. Brucken,[46] E. Bruna,[111] G. E. Bruno,[32] D. Budnikov,[100] H. Buesching,[61] S. Bufalino,[26,35] P. Buncic,[35] O. Busch,[129] Z. Buthelezi,[66] J. B. Butt,[16] J. T. Buxton,[19] J. Cabala,[116] D. Caffarri,[35] X. Cai,[7] H. Caines,[138] L. Calero Diaz,[73] A. Caliva,[54] E. Calvo Villar,[103] P. Camerini,[25] F. Carena,[35] W. Carena,[35] F. Carnesecchi,[27] J. Castillo Castellanos,[15] A. J. Castro,[126] E. A. R. Casula,[24] C. Ceballos Sanchez,[9] J. Cepila,[39] P. Cerello,[111] J. Cerkala,[116] B. Chang,[124] S. Chapeland,[35] M. Chartier,[125] J. L. Charvet,[15] S. Chattopadhyay,[134] S. Chattopadhyay,[101] A. Chauvin,[36,95] V. Chelnokov,[3] M. Cherney,[88] C. Cheshkov,[131] B. Cheynis,[131] V. Chibante Barroso,[35] D. D. Chinellato,[122] S. Cho,[51] P. Chochula,[35] K. Choi,[97] M. Chojnacki,[82] S. Choudhury,[134] P. Christakoglou,[83] C. H. Christensen,[82] P. Christiansen,[33] T. Chujo,[129] S. U. Chung,[97] C. Cicalo,[106] L. Cifarelli,[12,27] F. Cindolo,[105] J. Cleymans,[91] F. Colamaria,[32] D. Colella,[35,56] A. Collu,[75] M. Colocci,[27] G. Conesa Balbastre,[72] Z. Conesa del Valle,[52] M. E. Connors,[138,‡] J. G. Contreras,[39] T. M. Cormier,[86] Y. Corrales Morales,[26,111] I. Cortés Maldonado,[2] P. Cortese,[31] M. R. Cosentino,[121] F. Costa,[35] P. Crochet,[71] R. Cruz Albino,[11] E. Cuautle,[63] L. Cunqueiro,[35,62] T. Dahms,[36,95] A. Dainese,[108] M. C. Danisch,[94] A. Danu,[59] D. Das,[101] I. Das,[101] S. Das,[4] A. Dash,[80] S. Dash,[48] S. De,[121] A. De Caro,[12,30] G. de Cataldo,[104] C. de Conti,[121] J. de Cuveland,[42] A. De Falco,[24] D. De Gruttola,[12,30] N. De Marco,[111] S. De Pasquale,[30] R. D. De Souza,[122] A. Deisting,[94,98] A. Deloff,[78] E. Dénes,[137,†] C. Deplano,[83] P. Dhankher,[48] D. Di Bari,[32] A. Di Mauro,[35] P. Di Nezza,[73] B. Di Ruzza,[108] M. A. Diaz Corchero,[10] T. Dietel,[91] P. Dillenseger,[61] R. Divià,[35] Ø. Djuvsland,[22] A. Dobrin,[59,83] D. Domenicis Gimenez,[121] B. Dönigus,[61] O. Dordic,[21] T. Drozhzhova,[61] A. K. Dubey,[134] A. Dubla,[54] L. Ducroux,[131] P. Dupieux,[71] R. J. Ehlers,[138] D. Elia,[104] E. Endress,[103] H. Engel,[60] E. Epple,[36,95,138] B. Erazmus,[114] I. Erdemir,[61] F. Erhardt,[130] B. Espagnon,[52] M. Estienne,[114] S. Esumi,[129] J. Eum,[97] D. Evans,[102] S. Evdokimov,[112] G. Eyyubova,[39] L. Fabbietti,[36,95] D. Fabris,[108] J. Faivre,[72] A. Fantoni,[73] M. Fasel,[75] L. Feldkamp,[62] A. Feliciello,[111] G. Feofilov,[133] J. Ferencei,[85] A. Fernández Téllez,[2] E. G. Ferreiro,[17] A. Ferretti,[26] A. Festanti,[29] V. J. G. Feuillard,[15,71] J. Figiel,[118] M. A. S. Figueredo,[121,125] S. Filchagin,[100] D. Finogeev,[53] F. M. Fionda,[24] E. M. Fiore,[32] M. G. Fleck,[94] M. Floris,[35] S. Foertsch,[66] P. Foka,[98] S. Fokin,[81] E. Fragiacomo,[110] A. Francescon,[29,35] A. Francisco,[114] U. Frankenfeld,[98] G. G. Fronze,[26] U. Fuchs,[35] C. Furget,[72] A. Furs,[53] M. Fusco Girard,[30] J. J. Gaardhøje,[82] M. Gagliardi,[26] A. M. Gago,[103] K. Gajdosova,[82] M. Gallio,[26] C. D. Galvan,[120] D. R. Gangadharan,[75] P. Ganoti,[90] C. Gao,[7] C. Garabatos,[98] E. Garcia-Solis,[13] C. Gargiulo,[35] P. Gasik,[36,95] E. F. Gauger,[119] M. Germain,[114] M. Gheata,[35,59] P. Ghosh,[134] S. K. Ghosh,[4] P. Gianotti,[73] P. Giubellino,[35,111] P. Giubilato,[29] E. Gladysz-Dziadus,[118] P. Glässel,[94] D. M. Gómez Coral,[64] A. Gomez Ramirez,[60] A. S. Gonzalez,[35] V. Gonzalez,[10] P. González-Zamora,[10] S. Gorbunov,[42] L. Görlich,[118] S. Gotovac,[117] V. Grabski,[64] O. A. Grachov,[138] L. K. Graczykowski,[135] K. L. Graham,[102] A. Grelli,[54] A. Grigoras,[35] C. Grigoras,[35] V. Grigoriev,[76] A. Grigoryan,[1] S. Grigoryan,[67] B. Grinyov,[3] N. Grion,[110] J. M. Gronefeld,[98] J. F. Grosse-Oetringhaus,[35] R. Grosso,[98] L. Gruber,[113] F. Guber,[53] R. Guernane,[72] B. Guerzoni,[27] K. Gulbrandsen,[82] T. Gunji,[128] A. Gupta,[92] R. Gupta,[92] R. Haake,[35] Ø. Haaland,[22] C. Hadjidakis,[52] M. Haiduc,[59] H. Hamagaki,[128] G. Hamar,[137] J. C. Hamon,[65] J. W. Harris,[138] A. Harton,[13] D. Hatzifotiadou,[105] S. Hayashi,[128] S. T. Heckel,[61] E. Hellbär,[61] H. Helstrup,[37] A. Herghelegiu,[79] G. Herrera Corral,[11] B. A. Hess,[34] K. F. Hetland,[37] H. Hillemanns,[35] B. Hippolyte,[65] D. Horak,[39] R. Hosokawa,[129] P. Hristov,[35] C. Hughes,[126] T. J. Humanic,[19] N. Hussain,[44] T. Hussain,[18] D. Hutter,[42] D. S. Hwang,[20] R. Ilkaev,[100] M. Inaba,[129] E. Incani,[24] M. Ippolitov,[76,81] M. Irfan,[18] M. Ivanov,[98] V. Ivanov,[87] V. Izucheev,[112] B. Jacak,[75] N. Jacazio,[27] P. M. Jacobs,[75] M. B. Jadhav,[48] S. Jadlovska,[116] J. Jadlovsky,[56,116] C. Jahnke,[121] M. J. Jakubowska,[135] H. J. Jang,[69] M. A. Janik,[135] P. H. S. Y. Jayarathna,[123] C. Jena,[29] S. Jena,[123] R. T. Jimenez Bustamante,[98] P. G. Jones,[102] A. Jusko,[102] P. Kalinak,[56] A. Kalweit,[35] J. Kamin,[61] J. H. Kang,[139] V. Kaplin,[76] S. Kar,[134] A. Karasu Uysal,[70] O. Karavichev,[53] T. Karavicheva,[53] L. Karayan,[94,98] E. Karpechev,[53] U. Kebschull,[60]

R. Keidel,[140] D. L. D. Keijdener,[54] M. Keil,[35] M. Mohisin Khan,[18,§] P. Khan,[101] S. A. Khan,[134] A. Khanzadeev,[87] Y. Kharlov,[112] B. Kileng,[37] D. W. Kim,[43] D. J. Kim,[124] D. Kim,[139] H. Kim,[139] J. S. Kim,[43] J. Kim,[94] M. Kim,[139] S. Kim,[20] T. Kim,[139] S. Kirsch,[42] I. Kisel,[42] S. Kiselev,[55] A. Kisel,[135] G. Kiss,[137] J. L. Klay,[6] C. Klein,[61] J. Klein,[35] C. Klein-Bösing,[62] S. Klewin,[94] A. Kluge,[35] M. L. Knichel,[94] A. G. Knospe,[119,123] C. Kobdaj,[115] M. Kofarago,[35] T. Kollegger,[98] A. Kolojvari,[133] V. Kondratiev,[133] N. Kondratyeva,[76] E. Kondratyuk,[112] A. Konevskikh,[53] M. Kopcik,[116] M. Kour,[92] C. Kouzinopoulos,[35] O. Kovalenko,[78] V. Kovalenko,[133] M. Kowalski,[118] G. Koyithatta Meethaleveedu,[48] I. Králik,[56] A. Kravčáková,[40] M. Krivda,[56,102] F. Krizek,[85] E. Kryshen,[35,87] M. Krzewicki,[42] A. M. Kubera,[19] V. Kučera,[85] C. Kuhn,[65] P. G. Kuijer,[83] A. Kumar,[92] J. Kumar,[48] L. Kumar,[89] S. Kumar,[48] P. Kurashvili,[78] A. Kurepin,[53] A. B. Kurepin,[53] A. Kuryakin,[100] M. J. Kweon,[51] Y. Kwon,[139] S. L. La Pointe,[111] P. La Rocca,[28] P. Ladron de Guevara,[11] C. Lagana Fernandes,[121] I. Lakomov,[35] R. Langoy,[41] K. Lapidus,[36,95] C. Lara,[60] A. Lardeux,[15] A. Lattuca,[26] E. Laudi,[35] R. Lea,[25] L. Leardini,[94] G. R. Lee,[102] S. Lee,[139] F. Lehas,[83] S. Lehner,[113] R. C. Lemmon,[84] V. Lenti,[104] E. Leogrande,[54] I. León Monzón,[120] H. León Vargas,[64] M. Leoncino,[26] P. Lévai,[137] S. Li,[7,71] X. Li,[14] J. Lien,[41] R. Lietava,[102] S. Lindal,[21] V. Lindenstruth,[42] C. Lippmann,[98] M. A. Lisa,[19] H. M. Ljunggren,[33] D. F. Lodato,[54] P. I. Loenne,[22] V. Loginov,[76] C. Loizides,[75] X. Lopez,[71] E. López Torres,[9] A. Lowe,[137] P. Luettig,[61] M. Lunardon,[29] G. Luparello,[25] T. H. Lutz,[138] A. Maevskaya,[53] M. Mager,[35] S. Mahajan,[92] S. M. Mahmood,[21] A. Maire,[65] R. D. Majka,[138] M. Malaev,[87] I. Maldonado Cervantes,[63] L. Malinina,[67,‖] D. Mal'Kevich,[55] P. Malzacher,[98] A. Mamonov,[100] V. Manko,[81] F. Manso,[71] V. Manzari,[35,104] M. Marchisone,[26,66,127] J. Mareš,[57] G. V. Margagliotti,[25] A. Margotti,[105] J. Margutti,[54] A. Marín,[98] C. Markert,[119] M. Marquard,[61] N. A. Martin,[98] J. Martin Blanco,[114] P. Martinengo,[35] M. I. Martínez,[2] G. Martínez García,[114] M. Martinez Pedreira,[35] A. Mas,[121] S. Masciocchi,[98] M. Masera,[26] A. Masoni,[106] A. Mastroserio,[32] A. Matyja,[118] C. Mayer,[118] J. Mazer,[126] M. A. Mazzoni,[109] D. Mcdonald,[123] F. Meddi,[23] Y. Melikyan,[76] A. Menchaca-Rocha,[64] E. Meninno,[30] J. Mercado Pérez,[94] M. Meres,[38] Y. Miake,[129] M. M. Mieskolainen,[46] K. Mikhaylov,[55,67] L. Milano,[35,75] J. Milosevic,[21] A. Mischke,[54] A. N. Mishra,[49] D. Miśkowiec,[98] J. Mitra,[134] C. M. Mitu,[59] N. Mohammadi,[54] B. Mohanty,[80] L. Molnar,[65] L. Montaño Zetina,[11] E. Montes,[10] D. A. Moreira De Godoy,[62] L. A. P. Moreno,[2] S. Moretto,[29] A. Morreale,[114] A. Morsch,[35] V. Muccifora,[73] E. Mudnic,[117] D. Mühlheim,[62] S. Muhuri,[134] M. Mukherjee,[134] J. D. Mulligan,[138] M. G. Munhoz,[121] K. Münning,[45] R. H. Munzer,[36,61,95] H. Murakami,[128] S. Murray,[66] L. Musa,[35] J. Musinsky,[56] B. Naik,[48] R. Nair,[78] B. K. Nandi,[48] R. Nania,[105] E. Nappi,[104] M. U. Naru,[16] H. Natal da Luz,[121] C. Nattrass,[126] S. R. Navarro,[2] K. Nayak,[80] R. Nayak,[48] T. K. Nayak,[134] S. Nazarenko,[100] A. Nedosekin,[55] L. Nellen,[63] F. Ng,[123] M. Nicassio,[98] M. Niculescu,[59] J. Niedziela,[35] B. S. Nielsen,[82] S. Nikolaev,[81] S. Nikulin,[81] V. Nikulin,[87] F. Noferini,[12,105] P. Nomokonov,[67] G. Nooren,[54] J. C. C. Noris,[2] J. Norman,[125] A. Nyanin,[81] J. Nystrand,[22] H. Oeschler,[94] S. Oh,[138] S. K. Oh,[68] A. Ohlson,[35] A. Okatan,[70] T. Okubo,[47] J. Oleniacz,[135] A. C. Oliveira Da Silva,[121] M. H. Oliver,[138] J. Onderwaater,[98] C. Oppedisano,[111] R. Orava,[46] M. Oravec,[116] A. Ortiz Velasquez,[63] A. Oskarsson,[33] J. Otwinowski,[118] K. Oyama,[77,94] M. Ozdemir,[61] Y. Pachmayer,[94] D. Pagano,[132] P. Pagano,[30] G. Paić,[63] S. K. Pal,[134] J. Pan,[136] A. K. Pandey,[48] V. Papikyan,[1] G. S. Pappalardo,[107] P. Pareek,[49] W. J. Park,[98] S. Parmar,[89] A. Passfeld,[62] V. Paticchio,[104] R. N. Patra,[134] B. Paul,[101,111] H. Pei,[7] T. Peitzmann,[54] X. Peng,[7] H. Pereira Da Costa,[15] D. Peresunko,[76,81] E. Perez Lezama,[61] V. Peskov,[61] Y. Pestov,[5] V. Petráček,[39] V. Petrov,[112] M. Petrovici,[79] C. Petta,[28] S. Piano,[110] M. Pikna,[38] P. Pillot,[114] L. O. D. L. Pimentel,[82] O. Pinazza,[35,105] L. Pinsky,[123] D. B. Piyarathna,[123] M. Płoskoń,[75] M. Planinic,[130] J. Pluta,[135] S. Pochybova,[137] P. L. M. Podesta-Lerma,[120] M. G. Poghosyan,[86,88] B. Polichtchouk,[112] N. Poljak,[130] W. Poonsawat,[115] A. Pop,[79] H. Poppenborg,[62] S. Porteboeuf-Houssais,[71] J. Porter,[75] J. Pospisil,[85] S. K. Prasad,[4] R. Preghenella,[35,105] F. Prino,[111] C. A. Pruneau,[136] I. Pshenichnov,[53] M. Puccio,[26] G. Puddu,[24] P. Pujahari,[136] V. Punin,[100] J. Putschke,[136] H. Qvigstad,[21] A. Rachevski,[110] S. Raha,[4] S. Rajput,[92] J. Rak,[124] A. Rakotozafindrabe,[15] L. Ramello,[31] F. Rami,[65] R. Raniwala,[93] S. Raniwala,[93] S. S. Räsänen,[46] B. T. Rascanu,[61] D. Rathee,[89] K. F. Read,[86,126] K. Redlich,[78] R. J. Reed,[136] A. Rehman,[22] P. Reichelt,[61] F. Reidt,[35,94] X. Ren,[7] R. Renfordt,[61] A. R. Reolon,[73] A. Reshetin,[53] K. Reygers,[94] V. Riabov,[87] R. A. Ricci,[74] T. Richert,[33] M. Richter,[21] P. Riedler,[35] W. Riegler,[35] F. Riggi,[28] C. Ristea,[59] E. Rocco,[54] M. Rodríguez Cahuantzi,[2] A. Rodriguez Manso,[83] K. Røed,[21] E. Rogochaya,[67] D. Rohr,[42] D. Röhrich,[22] F. Ronchetti,[35,73] L. Ronflette,[114] P. Rosnet,[71] A. Rossi,[29] F. Roukoutakis,[90] A. Roy,[49] C. Roy,[65] P. Roy,[101] A. J. Rubio Montero,[10] R. Rui,[25] R. Russo,[26] E. Ryabinkin,[81] Y. Ryabov,[87] A. Rybicki,[118] S. Saarinen,[46] S. Sadhu,[134] S. Sadovsky,[112] K. Šafařík,[35] B. Sahlmuller,[61] P. Sahoo,[49] R. Sahoo,[49] S. Sahoo,[58] P. K. Sahu,[58] J. Saini,[134] S. Sakai,[73] M. A. Saleh,[136] J. Salzwedel,[19] S. Sambyal,[92] V. Samsonov,[76,87] L. Šándor,[56] A. Sandoval,[64] M. Sano,[129] D. Sarkar,[134] N. Sarkar,[134] P. Sarma,[44] E. Scapparone,[105] F. Scarlassara,[29] C. Schiaua,[79] R. Schicker,[94] C. Schmidt,[98] H. R. Schmidt,[34] M. Schmidt,[34] S. Schuchmann,[61] J. Schukraft,[35] M. Schulc,[39]

Y. Schutz,[35,114] K. Schwarz,[98] K. Schweda,[98] G. Scioli,[27] E. Scomparin,[111] R. Scott,[126] M. Šefčík,[40] J. E. Seger,[88]
Y. Sekiguchi,[128] D. Sekihata,[47] I. Selyuzhenkov,[98] K. Senosi,[66] S. Senyukov,[3,35] E. Serradilla,[10,64] A. Sevcenco,[59]
A. Shabanov,[53] A. Shabetai,[114] O. Shadura,[3] R. Shahoyan,[35] M. I. Shahzad,[16] A. Shangaraev,[112] A. Sharma,[92] M. Sharma,[92]
M. Sharma,[92] N. Sharma,[126] A. I. Sheikh,[134] K. Shigaki,[47] Q. Shou,[7] K. Shtejer,[9,26] Y. Sibiriak,[81] S. Siddhanta,[106]
K. M. Sielewicz,[35] T. Siemiarczuk,[78] D. Silvermyr,[33] C. Silvestre,[72] G. Simatovic,[130] G. Simonetti,[35] R. Singaraju,[134]
R. Singh,[80] V. Singhal,[134] T. Sinha,[101] B. Sitar,[38] M. Sitta,[31] T. B. Skaali,[21] M. Slupecki,[124] N. Smirnov,[138]
R. J. M. Snellings,[54] T. W. Snellman,[124] J. Song,[97] M. Song,[139] Z. Song,[7] F. Soramel,[29] S. Sorensen,[126] F. Sozzi,[98]
M. Spacek,[39] E. Spiriti,[73] I. Sputowska,[118] M. Spyropoulou-Stassinaki,[90] J. Stachel,[94] I. Stan,[59] P. Stankus,[86] E. Stenlund,[33]
G. Steyn,[66] J. H. Stiller,[94] D. Stocco,[114] P. Strmen,[38] A. A. P. Suaide,[121] T. Sugitate,[47] C. Suire,[52] M. Suleymanov,[16]
M. Suljic,[25,†] R. Sultanov,[55] M. Šumbera,[85] S. Sumowidagdo,[50] A. Szabo,[38] I. Szarka,[38] A. Szczepankiewicz,[135]
M. Szymanski,[135] U. Tabassam,[16] J. Takahashi,[122] G. J. Tambave,[22] N. Tanaka,[129] M. Tarhini,[52] M. Tariq,[18] M. G. Tarzila,[79]
A. Tauro,[35] G. Tejeda Muñoz,[2] A. Telesca,[35] K. Terasaki,[128] C. Terrevoli,[29] B. Teyssier,[131] J. Thäder,[75] D. Thakur,[49]
D. Thomas,[119] R. Tieulent,[131] A. Tikhonov,[53] A. R. Timmins,[123] A. Toia,[61] S. Trogolo,[26] G. Trombetta,[32] V. Trubnikov,[3]
W. H. Trzaska,[124] T. Tsuji,[128] A. Tumkin,[100] R. Turrisi,[108] T. S. Tveter,[21] K. Ullaland,[22] A. Uras,[131] G. L. Usai,[24]
A. Utrobicic,[130] M. Vala,[56] L. Valencia Palomo,[71] S. Vallero,[26] J. Van Der Maarel,[54] J. W. Van Hoorne,[35,113]
M. van Leeuwen,[54] T. Vanat,[85] P. Vande Vyvre,[35] D. Varga,[137] A. Vargas,[2] M. Vargyas,[124] R. Varma,[48] M. Vasileiou,[90]
A. Vasiliev,[81] A. Vauthier,[72] O. Vázquez Doce,[36,95] V. Vechernin,[133] A. M. Veen,[54] M. Veldhoen,[54] A. Velure,[22]
E. Vercellin,[26] S. Vergara Limón,[2] R. Vernet,[8] M. Verweij,[136] L. Vickovic,[117] J. Viinikainen,[124] Z. Vilakazi,[127]
O. Villalobos Baillie,[102] A. Villatoro Tello,[2] A. Vinogradov,[81] L. Vinogradov,[133] Y. Vinogradov,[100,†] T. Virgili,[30]
V. Vislavicius,[33] Y. P. Viyogi,[134] A. Vodopyanov,[67] M. A. Völkl,[94] K. Voloshin,[55] S. A. Voloshin,[136] G. Volpe,[32,137]
B. von Haller,[35] I. Vorobyev,[36,95] D. Vranic,[35,98] J. Vrláková,[40] B. Vulpescu,[71] B. Wagner,[22] J. Wagner,[98] H. Wang,[54]
M. Wang,[7] D. Watanabe,[129] Y. Watanabe,[128] M. Weber,[35,113] S. G. Weber,[98] D. F. Weiser,[94] J. P. Wessels,[62] U. Westerhoff,[62]
A. M. Whitehead,[91] J. Wiechula,[34] J. Wikne,[21] G. Wilk,[78] J. Wilkinson,[94] M. C. S. Williams,[105] B. Windelband,[94]
M. Winn,[94] P. Yang,[7] S. Yano,[47] Z. Yasin,[16] Z. Yin,[7] H. Yokoyama,[129] I.-K. Yoo,[97] J. H. Yoon,[51] V. Yurchenko,[3]
A. Zaborowska,[135] V. Zaccolo,[82] A. Zaman,[16] C. Zampolli,[35,105] H. J. C. Zanoli,[121] S. Zaporozhets,[67] N. Zardoshti,[102]
A. Zarochentsev,[133] P. Závada,[57] N. Zaviyalov,[100] H. Zbroszczyk,[135] I. S. Zgura,[59] M. Zhalov,[87] H. Zhang,[7,22] X. Zhang,[7,75]
Y. Zhang,[7] C. Zhang,[54] Z. Zhang,[7] C. Zhao,[21] N. Zhigareva,[55] D. Zhou,[7] Y. Zhou,[82] Z. Zhou,[22] H. Zhu,[7,22] J. Zhu,[7,114]
A. Zichichi,[12,27] A. Zimmermann,[94] M. B. Zimmermann,[35,62] G. Zinovjev,[3] and M. Zyzak[42]

(ALICE Collaboration)

[1]*A.I. Alikhanyan National Science Laboratory (Yerevan Physics Institute) Foundation, Yerevan, Armenia*
[2]*Benemérita Universidad Autónoma de Puebla, Puebla, Mexico*
[3]*Bogolyubov Institute for Theoretical Physics, Kiev, Ukraine*
[4]*Bose Institute, Department of Physics and Centre for Astroparticle Physics and Space Science (CAPSS), Kolkata, India*
[5]*Budker Institute for Nuclear Physics, Novosibirsk, Russia*
[6]*California Polytechnic State University, San Luis Obispo, California, USA*
[7]*Central China Normal University, Wuhan, China*
[8]*Centre de Calcul de l'IN2P3, Villeurbanne, France*
[9]*Centro de Aplicaciones Tecnológicas y Desarrollo Nuclear (CEADEN), Havana, Cuba*
[10]*Centro de Investigaciones Energéticas Medioambientales y Tecnológicas (CIEMAT), Madrid, Spain*
[11]*Centro de Investigación y de Estudios Avanzados (CINVESTAV), Mexico City and Mérida, Mexico*
[12]*Centro Fermi—Museo Storico della Fisica e Centro Studi e Ricerche "Enrico Fermi", Rome, Italy*
[13]*Chicago State University, Chicago, Illinois, USA*
[14]*China Institute of Atomic Energy, Beijing, China*
[15]*Commissariat à l'Energie Atomique, IRFU, Saclay, France*
[16]*COMSATS Institute of Information Technology (CIIT), Islamabad, Pakistan*
[17]*Departamento de Física de Partículas and IGFAE, Universidad de Santiago de Compostela, Santiago de Compostela, Spain*
[18]*Department of Physics, Aligarh Muslim University, Aligarh, India*
[19]*Department of Physics, Ohio State University, Columbus, Ohio, USA*
[20]*Department of Physics, Sejong University, Seoul, South Korea*
[21]*Department of Physics, University of Oslo, Oslo, Norway*

[22]Department of Physics and Technology, University of Bergen, Bergen, Norway
[23]Dipartimento di Fisica dell'Università 'La Sapienza' and Sezione INFN Rome, Italy
[24]Dipartimento di Fisica dell'Università and Sezione INFN, Cagliari, Italy
[25]Dipartimento di Fisica dell'Università and Sezione INFN, Trieste, Italy
[26]Dipartimento di Fisica dell'Università and Sezione INFN, Turin, Italy
[27]Dipartimento di Fisica e Astronomia dell'Università and Sezione INFN, Bologna, Italy
[28]Dipartimento di Fisica e Astronomia dell'Università and Sezione INFN, Catania, Italy
[29]Dipartimento di Fisica e Astronomia dell'Università and Sezione INFN, Padova, Italy
[30]Dipartimento di Fisica 'E.R. Caianiello' dell'Università and Gruppo Collegato INFN, Salerno, Italy
[31]Dipartimento di Scienze e Innovazione Tecnologica dell'Università del Piemonte Orientale and Gruppo Collegato INFN,
Alessandria, Italy
[32]Dipartimento Interateneo di Fisica 'M. Merlin' and Sezione INFN, Bari, Italy
[33]Division of Experimental High Energy Physics, University of Lund, Lund, Sweden
[34]Eberhard Karls Universität Tübingen, Tübingen, Germany
[35]European Organization for Nuclear Research (CERN), Geneva, Switzerland
[36]Excellence Cluster Universe, Technische Universität München, Munich, Germany
[37]Faculty of Engineering, Bergen University College, Bergen, Norway
[38]Faculty of Mathematics, Physics and Informatics, Comenius University, Bratislava, Slovakia
[39]Faculty of Nuclear Sciences and Physical Engineering, Czech Technical University in Prague,
Prague, Czech Republic
[40]Faculty of Science, P.J. Šafárik University, Košice, Slovakia
[41]Faculty of Technology, Buskerud and Vestfold University College, Vestfold, Norway
[42]Frankfurt Institute for Advanced Studies, Johann Wolfgang Goethe-Universität Frankfurt, Frankfurt, Germany
[43]Gangneung-Wonju National University, Gangneung, South Korea
[44]Gauhati University, Department of Physics, Guwahati, India
[45]Helmholtz-Institut für Strahlen- und Kernphysik, Rheinische Friedrich-Wilhelms-Universität Bonn, Bonn, Germany
[46]Helsinki Institute of Physics (HIP), Helsinki, Finland
[47]Hiroshima University, Hiroshima, Japan
[48]Indian Institute of Technology Bombay (IIT), Mumbai, India
[49]Indian Institute of Technology Indore, Indore (IITI), India
[50]Indonesian Institute of Sciences, Jakarta, Indonesia
[51]Inha University, Incheon, South Korea
[52]Institut de Physique Nucléaire d'Orsay (IPNO), Université Paris-Sud, CNRS-IN2P3, Orsay, France
[53]Institute for Nuclear Research, Academy of Sciences, Moscow, Russia
[54]Institute for Subatomic Physics of Utrecht University, Utrecht, The Netherlands
[55]Institute for Theoretical and Experimental Physics, Moscow, Russia
[56]Institute of Experimental Physics, Slovak Academy of Sciences, Košice, Slovakia
[57]Institute of Physics, Academy of Sciences of the Czech Republic, Prague, Czech Republic
[58]Institute of Physics, Bhubaneswar, India
[59]Institute of Space Science (ISS), Bucharest, Romania
[60]Institut für Informatik, Johann Wolfgang Goethe-Universität Frankfurt, Frankfurt, Germany
[61]Institut für Kernphysik, Johann Wolfgang Goethe-Universität Frankfurt, Frankfurt, Germany
[62]Institut für Kernphysik, Westfälische Wilhelms-Universität Münster, Münster, Germany
[63]Instituto de Ciencias Nucleares, Universidad Nacional Autónoma de México, Mexico City, Mexico
[64]Instituto de Física, Universidad Nacional Autónoma de México, Mexico City, Mexico
[65]Institut Pluridisciplinaire Hubert Curien (IPHC), Université de Strasbourg, CNRS-IN2P3, Strasbourg, France
[66]iThemba LABS, National Research Foundation, Somerset West, South Africa
[67]Joint Institute for Nuclear Research (JINR), Dubna, Russia
[68]Konkuk University, Seoul, South Korea
[69]Korea Institute of Science and Technology Information, Daejeon, South Korea
[70]KTO Karatay University, Konya, Turkey
[71]Laboratoire de Physique Corpusculaire (LPC), Clermont Université, Université Blaise Pascal,
CNRS–IN2P3, Clermont-Ferrand, France
[72]Laboratoire de Physique Subatomique et de Cosmologie, Université Grenoble-Alpes,
CNRS-IN2P3, Grenoble, France
[73]Laboratori Nazionali di Frascati, INFN, Frascati, Italy
[74]Laboratori Nazionali di Legnaro, INFN, Legnaro, Italy
[75]Lawrence Berkeley National Laboratory, Berkeley, California, USA
[76]Moscow Engineering Physics Institute, Moscow, Russia
[77]Nagasaki Institute of Applied Science, Nagasaki, Japan

[78]National Centre for Nuclear Studies, Warsaw, Poland

[79]National Institute for Physics and Nuclear Engineering, Bucharest, Romania

[80]National Institute of Science Education and Research, Bhubaneswar, India

[81]National Research Centre Kurchatov Institute, Moscow, Russia

[82]Niels Bohr Institute, University of Copenhagen, Copenhagen, Denmark

[83]Nikhef, Nationaal instituut voor subatomaire fysica, Amsterdam, The Netherlands

[84]Nuclear Physics Group, STFC Daresbury Laboratory, Daresbury, United Kingdom

[85]Nuclear Physics Institute, Academy of Sciences of the Czech Republic, Řežu Prahy, Czech Republic

[86]Oak Ridge National Laboratory, Oak Ridge, Tennessee, USA

[87]Petersburg Nuclear Physics Institute, Gatchina, Russia

[88]Physics Department, Creighton University, Omaha, Nebraska, USA

[89]Physics Department, Panjab University, Chandigarh, India

[90]Physics Department, University of Athens, Athens, Greece

[91]Physics Department, University of Cape Town, Cape Town, South Africa

[92]Physics Department, University of Jammu, Jammu, India

[93]Physics Department, University of Rajasthan, Jaipur, India

[94]Physikalisches Institut, Ruprecht-Karls-Universität Heidelberg, Heidelberg, Germany

[95]Physik Department, Technische Universität München, Munich, Germany

[96]Purdue University, West Lafayette, Indiana, USA

[97]Pusan National University, Pusan, South Korea

[98]Research Division and ExtreMe Matter Institute EMMI, GSI Helmholtzzentrum für Schwerionenforschung, Darmstadt, Germany

[99]Rudjer Bošković Institute, Zagreb, Croatia

[100]Russian Federal Nuclear Center (VNIIEF), Sarov, Russia

[101]Saha Institute of Nuclear Physics, Kolkata, India

[102]School of Physics and Astronomy, University of Birmingham, Birmingham, United Kingdom

[103]Sección Física, Departamento de Ciencias, Pontificia Universidad Católica del Perú, Lima, Peru

[104]Sezione INFN, Bari, Italy

[105]Sezione INFN, Bologna, Italy

[106]Sezione INFN, Cagliari, Italy

[107]Sezione INFN, Catania, Italy

[108]Sezione INFN, Padova, Italy

[109]Sezione INFN, Rome, Italy

[110]Sezione INFN, Trieste, Italy

[111]Sezione INFN, Turin, Italy

[112]SSC IHEP of NRC Kurchatov Institute, Protvino, Russia

[113]Stefan Meyer Institut für Subatomare Physik (SMI), Vienna, Austria

[114]SUBATECH, Ecole des Mines de Nantes, Université de Nantes, CNRS-IN2P3, Nantes, France

[115]Suranaree University of Technology, Nakhon Ratchasima, Thailand

[116]Technical University of Košice, Košice, Slovakia

[117]Technical University of Split FESB, Split, Croatia

[118]The Henryk Niewodniczanski Institute of Nuclear Physics, Polish Academy of Sciences, Cracow, Poland

[119]The University of Texas at Austin, Physics Department, Austin, Texas, USA

[120]Universidad Autónoma de Sinaloa, Culiacán, Mexico

[121]Universidade de S ao Paulo (USP), Sao Paulo, Brazil

[122]Universidade Estadual de Campinas (UNICAMP), Campinas, Brazil

[123]University of Houston, Houston, Texas, USA

[124]University of Jyväskylä, Jyväskylä, Finland

[125]University of Liverpool, Liverpool, United Kingdom

[126]University of Tennessee, Knoxville, Tennessee, USA

[127]University of the Witwatersrand, Johannesburg, South Africa

[128]University of Tokyo, Tokyo, Japan

[129]University of Tsukuba, Tsukuba, Japan

[130]University of Zagreb, Zagreb, Croatia

[131]Université de Lyon, Université Lyon 1, CNRS/IN2P3, IPN-Lyon, Villeurbanne, France

[132]Università di Brescia, Brescia, Italy

[133]V. Fock Institute for Physics, St. Petersburg State University, St. Petersburg, Russia

[134]Variable Energy Cyclotron Centre, Kolkata, India

[135]Warsaw University of Technology, Warsaw, Poland

[136]Wayne State University, Detroit, Michigan, USA

[137]*Wigner Research Centre for Physics, Hungarian Academy of Sciences, Budapest, Hungary*
[138]*Yale University, New Haven, Connecticut, USA*
[139]*Yonsei University, Seoul, South Korea*
[140]*Zentrum für Technologietransfer und Telekommunikation (ZTT), Fachhochschule Worms, Worms, Germany*

[†]Deceased.
[‡]Also at Georgia State University, Atlanta, Georgia, USA.
[§]Also at Department of Applied Physics, Aligarh Muslim University, Aligarh, India.
[∥]Also at M.V. Lomonosov Moscow State University, D.V. Skobeltsyn Institute of Nuclear, Physics, Moscow, Russia.